2950 Niles Road, St. Joseph, MI 49085-9659, USA
269.429.0300 fax 269.429.3852 hq@asabe.org www.asabe.org

An ASABE Meeting Presentation

Paper Number: 131593414

Optimization of the Pyrolysis of Distillers Dried Grains with Solubles

Christine Wood[1], Kasiviswanathan Muthukumarappan[2], Kurt A. Rosentrater[3,]

[1] Graduate Research Assistant, SDSU, Dept. of Agricultural and Biosystems Engineering, SDSU North Campus Drive, Brookings, SD, 57006
[2] Professor, South Dakota State University, Dept. of Agricultural and Biosystems Engineering, SDSU North Campus Drive, Brookings, SD, 57007
[3] Iowa State University, Dept. of Agricultural and Biosystems Engineering 3167 NSRIC, Ames, IA, 50011, karosent@iastate.edu

Written for presentation at the

2013 ASABE Annual International Meeting

Sponsored by ASABE

Kansas City, Missouri

July 21 – 24, 2013

Abstract. As the quantity of distillers dried grains with solubles (DDGS) produced in the U.S. continues to expand, so too does the need for value-added applications. This study examined the use of extracting energy from DDGS using pyrolysis. Various pyrolysis parameters were used to produce bio-oil and bio-char from DDGS. Characterization of the bio-oil and bio-char included mass density, thermal conductivity, thermal diffusivity, apparent viscosity, and energy content and was used to determine optimal processing parameters. The bio-oil produced from DDGS was found to be comparable to bio-oils produced from other biomass, but also had some more desirable characteristics. Heating values were determined to range from 16.7 to 27.6 MJ/kg (7,200 to 11,800 Btu/lb), while the pH ranged from 4.2 to 5.5. The mass density of the bio-oils produced in this study ranged from 0.839 to 1.007 g/cm^3, which is lower than that of other known pyrolysis oils (1.16-1.28 g/cm^3). This type of application could expand the portfolio of coproduct uses, and thus improve the sustainability of the industry.

Keywords. Bio-char, Bio-oil, Distillers dried grains with solubles, DDGS, Pyrolysis, Thermochemical conversion

INTRODUCTION

In 2011, the ethanol industry produced a record 39 million metric tons of feed coproduct in the form of corn gluten meal (CGM), corn gluten feed (CGF), distillers dried grains with solubles (DDGS), and distillers wet grains (DWG) (RFA, 2012a). CGM and CGF are produced from non-fermentable materials (mainly protein, minerals, fat, and fiber) remaining after the production of ethanol by wet milling; while the dry grind process uses non-fermentable materials to produced DWG and DDGS. It is estimated that 88% of the ethanol produced in the United States is manufactured using dry grind methods, while the remaining 12% is produced from wet milling (RFA, 2010). Of the 39 million metric tons of feed produced in 2011, 92% was comprised of DDGS; this was an increase of nearly 32 million metric tons over the previous 10 years (2001-2011) (RFA, 2012a and RFA, 2012b).

DDGS is primarily used as a feed for livestock; the beef, dairy, swine, and poultry industries are the largest consumers, utilizing 99% of the product (RFA, 2012a). The remaining 1% is used as fillers in deicers, cat litter, lick barrels, and worm food (Bothast and Schlicher, 2005) or as feed supplements for goats, sheep, and fish (Kannadhason et al., 2010; RFA, 2012b; Rosentrater et al., 2009a; Rosentrater et al., 2009b; and Schaeffer et al., 2009). DDGS is an ideal feed ingredient for many animals because of its nutritional content; it is approximately 25% to 35% protein, 86.2% to 93.0% dry matter, 3% to 13% fat, and 7.2% fiber (Bhadra et al., 2009; Ganesan et al., 2008; Loy, 2008; Rosentrater and Muthukumarappan, 2006; Shurson and Alhamdi, 2008; and Weigel et al., 1997).

While a valuable feed ingredient, there are limitations on the demand of DDGS within the feed industry, primarily because fat and fiber content can limit the quantities at which it can be consumed by certain animals (Tiffany et al., 2008). If the production of DDGS continues to grow, there is a potential that supply may surpass the livestock industry's demand at some point. Thus value-added uses and new markets should be pursued to maintain the demand for coproducts (Rosentrater, 2007). Researchers have been studying the viability of DDGS within the human food market (Rosentrater, 2007; Rosentrater and Krishnan, 2006) and for the production of biodegradable plastics (Bothast and Schlicher, 2005; Tatara et al., 2006; Tatara et al., 2007).

In addition to being a protein- and fiber-dense material, DDGS is energy-dense and provides a significant source of energy to animal diets and other applications. Studies have shown that there is enough energy in DDGS that they could potentially be used to power ethanol plants (De Kam et al., 2007; Morey et al., 2006; Rosentrater, 2011; Tiffany et al., 2007). Wang et al. (2007), determined that approximately 25 MJ are present in every 1 kg DDGS, while only 1 MJ of electric energy and 10 MJ of thermal energy are required to produce 1 L of ethanol. The feasibility of using ethanol coproducts to provide energy for a 190 million L/y and a 380 million L/y dry grind ethanol plant was examined, and even if all the DDGS at each plant was used to generate process heat and energy for the facility, there would still be leftover energy which could

be sold to the grid, increasing the rate of return on investment for the facility (Tiffany et al., 2007).

This energy can be harvested from DDGS directly, by converting it to heat and power, or it can be converted into gaseous or liquid fuels to be used for energy production (Giuntoli et al., 2011). These conversions would most likely require some type of thermochemical conversion process, such as combustion, pyrolysis, or gasification (Wang et al., 2007). The main difference between these three processes is the presence of oxygen. Combustion occurs in the presence of full oxygen, while gasification occurs in the presence of partial oxygen, and pyrolysis occurs without oxygen.

The use of pyrolysis dates as far back as ancient Egypt where it was used to form tars for caulking boats and embalming agents. Today, thermochemical decomposition is used to convert organic matter into energy-dense oils, gasses, and carbon (Sadaka, 2009). There are two main types of pyrolysis, fast and slow, which are characterized based on their heating rate and product yield. Slow pyrolysis, also known as conventional pyrolysis, is very time consuming as it has a much lower heating rate, and has a very low bio-oil yield, while fast pyrolysis proceeds at a much faster rate, and turns the organic matter directly into a gaseous form, which is then condensed into bio-oil and hydrogen (Sadaka, 2009). For both slow and fast pyrolysis, parameters such as pressure and temperature can be varied. Pyrolysis produces a free flowing organic liquid, bio-oil; a solid carbon rich material, bio-char; and syngas. Most recently, pyrolysis is being explored as a way of turning biomass into liquid fuels (Babu and Chaurasia, 2003; Chao et al., 2005; Gheorghe, 2006; Sivasastri, 2013; Van de Velden et al., 2007).

While many studies have been conducted using corn cobs, corn stalks, straw, and other agricultural wastes for pyrolysis feedstock, little has been done to investigate the potential of utilizing distillers dried grains with solubles (DDGS) as a pyrolysis feedstock. Lei et al. (2011) and Giuntol (2011) are two of the few studies that have explored the potential use of DDGS in pyrolysis. Rosentrater (2011) provided a comprehensive overview of DDGS as a pyrolysis feedstock. In order to fully understand the potential for using pyrolysis to obtain energy from ethanol coproducts, this study examined various pyrolysis reaction parameters for conversion of DDGS, in order to optimize the production of liquid fuel.

MATERIALS AND METHODS

Sample Collection and Experimental Design

DDGS was obtained and stored in sealed plastic storage bags at room temperature (24±1^{o}C) until needed for pyrolysis. After processing the bio-oil collected was stored in plastic screw-top bottles in a refrigerator (6±1^{o}C) until analyzed. The bio-char was stored in sealed plastic storage bags at room temperature (24±1^{o}C) until analysis.

Pyrolysis reaction heating rates, times, and temperatures were varied among treatments (Table 1); two replicate pyrolysis reactions were performed per set of parameters (denoted as A and B), with the exception of the center point (600^{o}C, 40^{o}C/min, 2 h) which was replicated three times (A, B, and C). This resulted in a total of 19 samples (8 treatments replicated twice, the center point replicated three times). Three replicate measurements were then performed for each physical property measured (unless noted otherwise) on the bio-oils (thermal conductivity, thermal diffusivity, energy content, mass density, and apparent viscosity) and bio-chars (mass density, true density, particle size, and color). Rheology measurements were taken at three different temperatures (10, 20, and 40^{o}C, and again three replicates were taken for each treatment (19 samples x 3 temperatures).

Raw Material Composition

The carbon and nitrogen content for the raw materials was determined by an external laboratory (Servi-Tech Laboratories, Hastings, NE). The particle size distribution and color of the raw materials was determined using the same methods used for the bio-char, and are discussed subsequently.

Pyrolysis

The apparatus in Figure 1 (located in the SDSU bioprocessing laboratory) was used to perform slow pyrolysis reactions. Each reaction began with 500 g of sample in a sealed 6,589 cm^{3} (20 cm long with 10 cm internal diameter)steel chamber. The chamber was equipped with a purging inlet tube and an exhaust outlet leading to the distillation apparatus. The collection apparatus was comprised of four Allihn condenser columns with water jackets, and two glass bulbs (Chemglass Life Science, Vineland, NJ) to collect and sample the bio-oil. To assist with the condensation of oil, water cooled to 6^{o}C was cycled through the water jackets using an F3-V Refrigerated Cryostats (HAAKE, Paramus, NJ). The outlet after the fourth condenser was connected to hosing which released the produced syngas into a bucket of water to remove any additional condensable compounds before releasing the syngas into the air. The steel chamber was placed within an Isotemp Programmable muffle furnace (650-750, Fisher Scientific, Pittsburg, PA), which allowed the heating rate and temperature to be defined. Before heating, the chamber and distillation system were purged with nitrogen gas for 10 min in order to evacuate oxygen from the vessel.

For each pyrolysis reaction, the sealed vessel was heated to the specified temperature (500^{o}C, 600^{o}C, or 700^{o}C) at the specified heating rate (30^{o}C/min, 40^{o}C/min, and 50^{o}C/min), which were based on the experimental design in Table 1. Each pyrolysis reaction proceeded in three distinct steps: 1) moisture and some volatiles were removed from the feedstock; 2) more complex volatiles and some gasses were removed leaving bio-char; 3) bio-char was decomposed further and chemical rearrangement released more volatiles and gasses, producing a less reactive bio-char (Demirbas, 2004). The reaction was allowed to progress for a specified time (1.5, 2, and 2.5 h), based upon the experimental design (Table 1). At that point, the furnace was powered off and allowed to cool for 2 h before the bio-oil and bio-char were collected. When collected the mass of the bio-char and bio-oil were determined. These masses were compared to the mass of the

original feedstock sample in order to determine the mass yield (e.g. 100 x (mass bio-oil/mass feedstock) = yield bio-oil).

Bio-oils

Physical Properties

Thermal Properties and Energy Content

Thermal conductivity and diffusivity were determined for the bio-oil samples with a thermal properties meter (KD2, Decagon Devices, Pullman, WA) that utilized the line heat source probe technique (Baghe-Khandan et al., 1981). The lower heating values (LHV) of the bio-oil samples were measured using a bomb calorimeter (1341 Oxygen Bomb Calorimeter, Parr Instrument, Moline, IL). Two replications were completed for each bio-oil sample.

Density

Mass density for the bio-oil was determined using a specific gravity cup (Model H-38000-12, Cole-Parmer Instrument Co., Barrington, IL). Material was poured into the cup (mass = 83.55 g; volume = 83.2 cm^3), excess material was then removed, and the filled cup was weighed on a balance. Density was then calculated as the ratio of sample mass to sample volume.

Color

Color of the bio-oil was determined using a spectrophotocolorimeter (LabScan XE, Hunter Associates Laboratory, Reston, VA) using the Hunter Lab color space. L* value quantified the brightness/darkness of the samples; a* value depicted the redness/greenness; and b* value denoted the yellowness/blueness. Four measurements were made for each sample.

Viscosity

The apparent viscosity of the bio-oils was determined at three different temperatures in order to account for temperature variations that occur as the oils are moved and processed. Apparent viscosity is a fluid's resistance to flow when force is applied. It is expected (based on our previous work) that as either the shear rate or temperature are increased, the apparent viscosity of a fluid should decrease, and this relationship can be defined as a nonlinear power function represented by:

$$\eta = k\gamma^{n} \quad (1)$$

where η = apparent viscosity (Pa·s);

k = empirical regression constant (Pa·s·s);

γ = shear rate (1/s); and

n = empirical exponential constant (-).

Apparent viscosity was measured for the bio-oils using a rheometer (ATS Rheosystems, Rheologica Instruments Inc., NJ), using a cup and bob assembly. Approximately 15 mL of sample was placed into the cup, and the bob was used to apply shear rate at different speeds. The shear rate for each sample was initiated at 10 (s^{-1}), and was increased up to 200 (s^{-1}) by increments of approximately 5 (s^{-1}). Rheology measurements were also taken at three different temperatures (10, 20, and 40^{o}C).

Chemical Properties

Potential Hydrogen

The bio-oil's potential hydrogen (pH) was measured at room temperature (24±1^{o}C) using a digital pH meter (Fisher Scientific, Accumet model AB15).

GC-MS

Compound analysis was done using gas chromatography mass spectrometry (GC-MS) (Agilent Technologies, Santa Clara, CA) with an DB-5MS column (J&W Scientific, Inc., Folsom, CA), with a mobile phase of helium at a flow rate of 1.2 mL/min, and a sample volume of 1 μL. Samples were held for 2 min at 45^{o}C and then heated to 290^{o}C at 5^{o}C/min. They were then held for 5 min. Before running the samples through the GC-MS, the bio-oil samples were filtered through a 2 μm filter and then diluted with ethanol at 1:10, then again filtered through a 2 μm filter. Once the samples were run, product peaks were assigned specific compound names and quality values by an automatic National Institute of Standards and Technology (NIST) mass spectral library search.

Bio-chars

Physical Properties

Energy Content

Net energy content of the bio-char samples were measured using a bomb calorimeter (1260 Isoperibolic, Parr Instrument, Moline, IL). Two replications were completed for each char sample.

Density

Mass density for the bio-chars was determined using an 85 mL specific gravity cup (Model H-38000-12, Cole-Parmer Instrument Co., Barrington, IL). Material was poured into the cup, of a known mass and volume; excess material was then removed, and the filled cup was weighed on a balance. Density was then calculated as the ratio of mass to volume.

True density of the bio-char was determined using a multi-volume pycnometer (Model No. 1305, Micromeritics, Norcross, Georgia, USA). Calibration of the equipment was performed with a metal ball provided by the manufacturer. True density was determined by the volume displacement method using helium gas (Chang 1988). Then, using this measured true density and the measured mass density, the porosity of the bio-char was calculated using:

$$\phi = (\rho_t - \rho_m)/ \rho_t \text{ x } 100 \quad (2)$$

where

ϕ is porosity (%);

ρ_t is true density (g/cm^3); and

ρ_m is mass density (g/cm^3).

Particle Size

The particle size distribution of the bio-chars and raw material were measured using a Camsizer (Retsch Technology, Haan, Germany) with a digital image analysis tool. The distribution was defined based on three sizes within the entire population: d10, d50, d90. The d50 value is the median particle size within the population, with 50% of the population greater than this size, and 50% smaller than this size. Similarly, 10% of the population is smaller than the D10 size; while 90% of the population is smaller than the D90 size.

Color

Color of the bio-char was determined using a spectrophotocolorimeter (LabScan XE, Hunter Associates Laboratory, Reston, VA) using the Hunter Lab color space. L*, a*, and b* were as previously discussed. Four measurements were made for each experimental run.

Chemical Properties

Proximate Analysis

Proximate analysis of the raw materials as well as the bio-chars included the determination of moisture content, dry matter, total protein, and total nitrogen. These analyses were conducted externally by Servi-Tech Laboratories, Hastings, NE. The ash content of the bio-chars was determined following Standard Method 08-03 (AACC, 2000).

Data Analysis

Data analysis was completed for each test using Excel v. 2010 (Microsoft, Redmond, WA) software to determine mean values and standard deviations. Two-way analysis of variance was

conducted using general linear models using SAS (2004) V.8 (SAS Institute, Cary, NC), using a type I error rate (α) of 0.05, to determine main and interaction effects, and to identify least significant differences (LSD) between sample means, if differences were significant. Rheological data was modeled with the PROC NONLIN regression procedure in SAS.

RESULTS AND DISCUSSION

Bio-oils

The yield of bio-oil (Table 2) ranged from 18% (treatment 1) to 38% (treatments 6 & 9). The reported yield values for the bio-oil were, in fact, lower than the actual values due to some technical issues while collecting the entire sample. First, it was assumed that the condensation of the bio-oil was not 100% efficient and syngas left the system carrying some condensable liquids, and second, a small amount of bio-oil could not be transferred out of the condenser columns due to tar build up.

The yield from treatments 1 through 4 gradually increased from 16.98% to 20.56% showing that at 500^{o}C a heating rate of 50^{o}C/min produced a greater amount of bio-oil than 30^{o}C/min. It also shows that a longer retention time produced a greater amount of bio-oil. This same trend does not exist at 700^{o}C; however, the treatments at 700^{o}C produced greater quantities of bio-oil (average of 35.68%) than the treatments at 500 (average 30.27%) and 600^{o}C (average 19.14%).

Physical Properties

Thermal Properties and Energy Content

Thermal conductivity and diffusivity of the bio-oils can be found in Table 2. The thermal conductivities for the bio-oil ranged from 1.95 (treatment 2) to 4.38 W/m^{o}C (treatment 6). The conductivities of the oils produced at 700^{o}C were greater than those produced at 500^{o}C. The conductivity of common crude oils, 0.12 to 0.13 W/m^{o}C (0 to 50^{o}C) (Elam et al., 1989), is much lower than these values. Thermal diffusivity of the bio-oils produced in this study ranged from 0.092 (treatment 6) to 0.127 mm^{2} /s (treatment 1). The diffusivities of these oils are much lower than commonly used fuels: diesel fuel, 4.6 mm^{2}/s; ethanol, 10.0 mm^{2}/s; and gasoline, 6.4 mm^{2} /s (Waterland et al., 2003).

The lower heating value (LHV) for the bio-oils can be found in Table 2 as well. The LHV for the bio-oil ranged from 16.7 (7,200 Btu/lb) (treatment 2) to 27.6 MJ/kg (11,800 Btu/lb) (treatment 9). From the data presented, it appears that the LHV of the bio-oils increased as the process temperature increased. It also appears that as the heating rate and the retention time increased, the LHV also increased. The bio-oil produced from DDGS had LHV comparable to DDGS bio-oils produced in other studies (20 to 28 MJ/kg (Lei et al., 2011)), and are much lower than the LHV of other commonly used fuels: diesel 42.0 MJ/kg (18000 Btu/lb), ethanol 27.0 MJ/kg (12000 Btu/lb), and gasoline 43.9 MJ/kg (19000 Btu/lb) (Waterland et al., 2003). The heating values of other pyrolysis bio-oils have been found to range from 16 to 28 MJ/kg for various other feedstocks (wood,

rice husk, grasses, nut shells, seeds, etc.) (Ba et al., 2004; Bridgwater and Peacocke, 2000; Huang et al., 2008; Junming et al., 2008; Neves et al., 2011; Scholze, 2002), so other samples were similar.

Density

Generally, oils have densities less than that of water (1.0 g/cm^3); however, bio-oils do not always follow this behavior, and often have mass densities greater than 1.0. For example, the mass density of other pyrolysis bio-oils has ranged from 1.16 to1.28 g/cm^3 (Ba et al., 2004; Junming et al., 2008; and Scholze., 2002). It is most likely due to the tar present in the bio-oils that causes them to have densities greater than water. The mass densities of the bio-oils within this study fall both below and above that of water (1.00 g/cm^3). The mass density of the bio-oils produced at 500^{o}C had mass densities that ranged from 0.839 to 0.996 g/cm^3; while the bio-oils produced at 700^{o}C ranged from 0.998 to 1.007 g/cm^3, and that produced at 600^{o}C was 1.00 g/cm^3. These densities are much greater than those of commonly used fuels: diesel (0.863 g/cm^3), ethanol (0.785 g/cm^3), and gasoline (0.791 g/cm^3) (Waterland et al., 2003).

Color

The color of the bio-oils visually changed with the addition of more tar. The bio-oils with the greatest amounts of tar were the darkest in color. The L* a* and b* values of the bio-oils can be found in Table 3. The L* value quantified the brightness/ darkness of the samples, the larger the L* value the lighter the color, while the smaller the L* value the darker the color. As the processing temperature was increased from 500 to 700^{o}C the L* value decreased indicating that the sample became darker. By increasing time, heating rate, and temperature, the a* value decreased from 12.197 to 0.330. The b* values also decreased from 500 (average 2.980) to 700^{o}C (average 1.218).

Viscosity

The apparent viscosity of the bio-oils was determined at three different temperatures in order to determine the behavior of the oils under different processing conditions. Apparent viscosity measures a fluid's resistance to flow as force (or shear) is applied; when an increasing shear rate is applied the apparent viscosity of most oils remains constant, so they are considered Newtonian fluids. This is not the case for bio-oils, at least in their crude, unrefined states; so they are considered non-Newtonian. The DDGS-based bio-oil samples had viscosities that decreased with an increase in shear rate and an increase in temperature; this behavior is known as shear thinning. The relationship could be defined as a nonlinear power function represented by:

$$\eta = k\,\gamma^{n} \tag{3}$$

where

η = apparent viscosity (Pa·s);

k = empirical regression constant (Pa·s·s);

γ = shear rate (s^{-1}); and

n = empirical exponential constant (-).

The data collected from the apparent viscosity measurements for each treatment (i.e. each viscosity curve) were combined into a single linear regression in order to predict the overall behavior for each bio-oil at each of the three temperatures. The plots of these behaviors can be seen in Figures 2 and 3, and the overall average k and n regression values can be found in Table 4.

Comparing the viscosity curves from the different treatments, a few conclusions can be drawn. First, the temperature of the pyrolysis reaction has a visible effect on the initial viscosity of the bio-oils; the bio-oils produced at lower temperatures had a lower initial viscosity than those processed at higher temperatures. This was likely due to an increasing quantity of tar present in the bio-oil samples as temperature increased the bio-oil samples produced at lower temperatures had visibly less tar than those produced at higher temperatures.

Chemical Properties

Potential Hydrogen

The pH of the bio-oils in this study was found to range from 4.2 to 5.5 (Table 3). These values are only slightly higher than the pH values for most bio-oils produced via pyrolysis. For example, the pH of wood-based bio-oil produced by pyrolysis has been found to range from 2.4 to 3.5 (Ba et al., 2004; Sadaka, 2009; Scholze, 2002). Our higher pH values are actually a desirable characteristic, because in order to be utilized, the pH of the oil must be neutralized to reduce its corrosiveness.

Gas Chromatography-Mass Spectroscopy (GC-MS)

The bio-oils were also analyzed by GC-MS. While there were hundreds of compounds found within the bio-oil, only the most significant peaks were recorded. Table 5 lists the molecular formulas and potential compounds. The constituents of most bio-oils are complex, comprising mainly water, acids, alcohols, aldehydes, esters, ketones, and phenol derivatives.

Bio-chars

The yield of bio-chars ranged from 39% (treatment 8) to 77% (treatment 2). The bio-char yields were slightly higher than what was determined by Lei et al., (2011), where DDGS bio-char yields were determined to be 26% to 50%. It appears that the lower pyrolysis temperatures produced higher quantities of bio-char, yet there appears to be no correlation between the bio-char yield and retention time or heating rate.

Physical Properties

Energy Content

The lower heating values (LHV) of the bio-chars can be found in Table 7. The LHV for the bio-chars ranged from 23 (treatment 1) to 29 MJ/kg (treatment 5) (10,000 to 13,000 Btu/lb). Based on the heating values presented, it appears that the heating values of the bio-chars produced at 700^{o}C were greater than those of the bio-chars produced at 500^{o}C. However, the LHV of the bio-chars produced at 600^{o}C were the greatest of all.

Density

The mass density of the bio-char was determined to vary from 0.398 (treatment 6) to 0.514 g/cm^3 (treatment 5). This variance in mass density was most likely due to the variance in particle size of the bio-char. The mass density of the bio-char produced at 500^{o}C was greater than that produced at 700^{o}C; the mass density of the bio-char produced at 600^{o}C was greater than both. On average, the true density of the treatment 5 bio-char was determined to be 1.56 g/cm^3, while that of the treatment 8 bio-char was determined to be 1.87 g/cm^3. The porosity was determined to range from 70% (treatment 5) to 80% (treatment 8). The true density and porosity of the bio-char produced at 700^{o}C was greater than that produced at 500^{o}C, while the porosity of the bio-char produced at 600^{o}C was less than both.

Particle Size

The particle size of bio-char has an effect on packing density, as smaller particles have the potential to increase the bulk density of the material by decreasing the quantity of space required for storage. This has a large impact on storage and transport requirements for the material. It can also play a vital role in bio-char's particle-particle interactions as a soil amendment. A small particle size with large porosity may contribute the most to enhancing soil quality, while a large particle size could increase the stability of the carbon within the soil environment (Mullen et. al., 2010). The particle size for the bio-char can be found in Table 8. The median diameter for the bio-char ranged from 0.31 to 1.25 μm. From the data presented in Table 8 it appears that as the temperature of the pyrolysis reaction increased, the particle size of the bio-char decreased. It also appears that the longer the reaction was allowed to progress the smaller the particle size of the resulting bio-char.

Color

Bio-char can be used as a soil amendment, but when added to soils, it can darken the color of that soil. By darkening the soil, bio-char can increase a soil's ability to absorb more light energy, in turn increasing soil temperatures (Sohi et al., 2010). By increasing the soil temperature, the growing season can potentially be extended; it can also potentially accelerate nutrient cycling and accelerate snow melt (Sohi et al., 2010). The

color values for the bio-chars can be seen in Table 8. The L* values ranged from 9.28 to 12.68 and appeared to increase as the processing temperature and retention time was increased. The a* values from bio-char samples produced at 500^{o}C were greater than those produced at higher temperatures. No observable patterns between temperature/time and the b* value could be detected.

Chemical Properties

Proximate Analysis

The proximate compositions of the bio-chars produced from the pyrolysis reaction can be found in Table 6. The moisture content ranged from 1.6% (treatment 8) to 2.7% (treatment 2). Based on the data, it appears that as the pyrolysis temperature increased, the moisture content of the remaining char decreased. This was also true as the heating rate was reduced and the retention time was increased. The total carbon of the bio-chars ranged from 54 (treatment 2) to 64 mg/L (treatment 9); as the temperature of the pyrolysis reaction was increased so was the carbon content of the bio-char. All samples of bio-char had greater carbon content than the initial DDGS (46.56 % d.b.).

CONCLUSIONS

Record quantities of energy-dense DDGS are being produced by the U.S. fuel ethanol industry. This energy can potentially be harvested either directly or through slow pyrolysis, to produce bio-oils and bio-chars. The bio-oils produced in this study were determined to be similar to those produced from other biomaterials, but were also superior in some ways. For example, the pH of the bio-oils in this study was more favorable. Other properties may require upgrading for use as fuels or chemicals, including density, and apparent viscosity, and the heating values. In order to maximize the yield of both the bio-oil and bio-char, pyrolysis parameters must be set at a middle point, as a higher temperature and longer retention time yields greater oil but lower char. Similar to the yield, the bio-oil's heating value is maximized with higher temperatures, greater retention times, and higher heating rates. The bio-char's heating value is maximized at a mid-range temperature with a longer retention time and higher heating rate. So in order to maximize the heating values of both the bio-char and bio-oil, a mid-range temperature with higher heating rate and a greater retention time are required. It was also concluded that 500^{o}C was the best processing temperature when looking at viscosity; however, if the tar were to be removed from the bio-oil this may be changed.

ACKNOWLEDGEMENTS

The authors would like to thank Yijing Wang, Chinnadurai Karunanithy (CK), and Arulprakash Sivasastri for technical assistance with laboratory measurements

REFERENCES

AACC. 2000. *Approved Methods of the American Association of Cereal Chemists 10th ed.* St. Paul, MN: American Soc. of Cereal Chem.

Ba, T., A. Chaala, M. Garcia-Perez, D. Rodrique, and C. Roy. 2004. Colloidal properties of bio-oils obtained by vacuum pyrolysis of softwood bark. Characterization of water-soluble and water-insoluble fractions. *Energy Fuels* 18: 704-712.

Babu, B. V., and A. S. Chaurasia. 2003. Optimization of pyrolysis of biomass using differential evolution approach. In *Proc. of the Second Intl. Conf. on Computational Intelligence, Robotics, and Autonomous Syst.*, 787–792. Singapore: Computational Intelligence, Robotics, and Autonomous Systems.

Baghe-Khandan, M., S. Y. Choi, and M. R. Okos. 1981. Improved line heat source thermal conductivity probe. *J. Food Sci*. 46(5): 1430-1432

Bhadra, R., K. Muthukumarappan, and K. A. Rosentrater. 2009. Flowability properties of commercial distillers dried grains with solubles (DDGS). *Cereal Chem.* 86(2): 170-180.

Bothast, R., and M. Schlicher. 2005. Biotechnological processes for conversion of corn into ethanol. *Appl. Microbiology Biotechnology 67*: 19-25.

Bridgwater, A. V., and G. V. C. Peacocke. 2000. Fast pyrolysis processes for biomass. *Renewable Sustainable Energy Rev*. 4 (1): 1–73.

Chang, C. S. 1988. Measuring density and porosity of grain kernels using a gas pycnometer. *Cereal Chem.* 65(1): 13-15.

Chao, C., L. Qing, Y. Qiang, T. Kruttschnitt, and E. Pruckner. 2005. Comparative experiments on recycling of oil sludge, oil shale, and biomass waste in a continuous rotating pyrolysis reactor. In *Proc. 5th Asia-Pacific Conf. Combustion*, 51-54. Adelaide, Australia.

De Kam, M. J., R. V. Morey, and D. G. Tiffany. 2007. Integrating biomass to produce heat and power at ethanol plants. ASABE Paper No. 076232. St. Joseph, MI: ASABE.

Demirbas, A. 2004. Effects of temperature and particle size on bio-char yield from pyrolysis of agricultural residues. *J. Analytical Appl. Pyrolysis* 72(2004): 243-248.

Elam, S., I. Tokura, and K. Saito. 1989. Thermal conductivity of crude oils. *Exp. Thermal Fluid Sci.* 2(1): 1-6.

Ganesan, V., K. A. Rosentrater, and K. Muthukumarappan. 2008. Effect of flow agent addition on the physical properties of DDGS with varying moisture content and soluble levels. *Trans. ASABE* 51(2): 591-601.

Gheorghe, C. 2006. Investigations of potentialities of biomass pyrolysis at HTAG system. Bucharest, Romania: University of Bucharest, Power Engineering. Available at: http://www.energy.kth.se/proj/projects/SUSPOWER/Downloads/Report_Cora%20Gheorghe.pdf. Accessed 17 June 2013.

Giuntoli, J., J. Gout, A. Verkooijen, and W. De Jong. 2011. Characterization of fast pyrolysis of dry distillers grains (DDGS) and palm kernel cake using a heated foil reactor: nitrogen chemistry and basic reactor modeling. *Ind. Eng. Chem. Res.* 50(8): 4286-4300.

Huang, Y., W. Kuan, S. Lo, and C. Lin. 2008. Total recovery of resources and energy from rice straw using microwave-induced pyrolysis. *Bioresource Tech.* 99: 8252-8258.

Loy, D. 2008. Ethanol coproducts for cattle: the process and products. Ames, IA: Iowa State University, University Extension. Available at: http://www.extension.iastate.edu/publications/ibc18.pdf. Accessed 2 January 2012.

Junming, X., J. Jianchun, S. Yunjuan, and L. Yanju. 2008. Bio-oil upgrading by means of ethyl ester production in reactive distillation to remove water and to improve storage and fuel characteristics. *Biomass and Bioenergy* 32: 1056-1061.

Kannadhason, S., K. A. Rosentrater, and K. Muthukumarappan. 2010. Twin screw extrusion of DDGS based aquaculture feeds. *J. World Aquac. Soc*. 41: 1-15.

Lei, H., S. Ren, L. Wang, Q. Bu, J. Julson, J. Holladay, and R. Ruan. 2011. Microwave pyrolysis of distillers dried grain with solubles (DDGS) for biofuel production. *Bioresource Tech.* 102: 6208-6213.

Morey, R., D. Tiffany, and D. Hatfield. 2006. Biomass for electricity and process heat at ethanol plants. *Appl. Eng. Agric.* 22(5): 723-728.

Mullen, C., A. Boateng, N. Goldberg, I. Lima, D. Laird, and K. Hicks. 2010. Bio-oil and bio-char production from corn cobs and stover by fast pyrolysis. *Biomass Bioenergy* 34(2010): 67-74.

Neves, D., H. Thunman, A. Matos, L. Tarelho, and A. Gomez-Barea. 2011. Characterization and prediction of biomass pyrolysis products. *Progress Energy Combustion Sci.* 37: 611-630.

RFA (Renewable Fuels Association). 2010. Climate of opportunity: 2010 Industry Outlook. Washington, D.C.: Renewable Fuels Association. Available at: http://ethanolrfa.org/page/-/objects/pdf/outlook/RFAoutlook2010_fin.pdf. Accessed 12 February 2013.

RFA (Renewable Fuels Association). 2012a. Accelerating industry innovation, 2012 Ethanol Industry Outlook. Washington, D.C.: Renewable Fuels Association. Available at: http://ethanolrfa.3cdn.net/d4ad995ffb7ae8fbfe_1vm62ypzd.pdf. Accessed 17 Oct. 2012.

RFA (Renewable Fuels Association). 2012b. Industry Resources: Co-products. Washington, D.C.: Renewable Fuels Association. Available at: http://ethanolrfa.org/pages/industry-resources-coproducts. Accessed 24 October 2012.

Rosentrater, K. A. 2007. Corn ethanol coproducts – some current constraints and potential opportunities. *Int. Sugar J.* 109(1307): 2-11.

Rosentrater, K. A. 2011. Chapter 20, Using DDGS as a feedstock for bioenergy via thermochemical conversion. In *Distillers Grains: Production, Properties, and Utilization*, 449-463. K. Liu and K. A. Rosentrater, eds. Boca Raton, FL: CRC Press, Taylor and Francis.

Rosentrater, K. A., and K. Muthukumarappan. 2006. Corn ethanol coproducts: generation, properties, and future prospects. *Int. Sugar J.* 108(1295): 648-657.

Rosentrater, K. A., K. Muthukumarappan, and S. Kannadhason. 2009a. Effect of ingredients and extrusion parameters on aquafeeds containing DDGS and potato starch. *J. Aquac. Feed Sci. and Nutrition* 1(1): 22-38.

Rosentrater, K. A., K. Muthukumarappan, and S. Kannadhason. 2009b. Effect of ingredients and extrusion parameters on properties of aquafeeds containing DDGS and corn starch. *J. Aquac. Feed Sci. and Nutrition* 1(2): 44-60.

Rosentrater, K. A., and P. Krishnan. 2006. Incorporating distillers grains in food products. *Cereal Foods World.* 51(2): 52-60.

Sadaka, S. 2009. Chapter 2: Pyrolysis. In *Pyrolysis and Bio-Oil*. Fayetteville, AR: Cooperative Extension Services.

Schaeffer, T.W., M. L. Brown, and K. A. Rosentrater. 2009. Performance characteristics of Nile Tilapia (*Oreochromis niloticus*) fed diets containing graded levels of fuel based distillers' grains with solubles. *J. Aquac. Feed Sci. and Nutrition* 1(4): 78-83.

Schlicher, M. 2005. The flowability factor. *Ethanol Prod. Mag.* 11(7): 90-93, 110-111.

Scholze, B. 2002. Long-term stability, catalytic upgrading, and application of pyrolysis oils – improving the properties of a potential substitute for fossil fuels. PhD diss. Hamburg, Germany: Zur Erlangung des Doktorgrades im Fachbereich Chemie der Universitat.

Shurson, J. and A. S. Alhamdi. 2008. Quality and new technologies to create corn co-products from ethanol production. *Using Distillers Grains in the U.S. and International Livestock and Poultry Industries, 231-256.* B. A. Babcock, D. J. Hayes, and J. D. Lawrence, eds. Ames, IA: Iowa State University.

Sivasastri, A. 2013. Conventional pyrolysis of corn stover, prairie cord grass, and big blue stem using batch type pyrolysis unit. MS thesis. Brookings, South Dakota: South Dakota State University, Department of Agricultural and Biosystems Engineering.

Sohi, S. P., E. Krull, E. Lopez-Capel, and R. Bol. 2010. Chapter 2: A review of bio-char and its use and function in soil. In *Advances in Agronomy*, 47-82. D. L. Sparks, ed. Burlington, MA: Academic Press.

Tatara, R., K. A. Rosentrater, and S. Suraparaju. 2006. Design properties for molded, corn-based DDGS-filled phenolic resin. *Ind. Crops and Products* 29: 9-15.

Tatara, R., K. A. Rosentrater, and S. Suraparaju. 2007. Compression molding of phenolic resin and corn-based DDGS blends. *J. Polymer Environ.* 15: 89-95.

Tiffany, D., R. V. Morey, and M. De Kam. 2007. Economics of biomass gasification/combustion at fuel ethanol plants. *Appl. Eng. Agric.* 25(3): 391-400.

Tiffany, D., R. V. Morey, and M. De Kam. 2008. Use of distillers by-products and corn stover as fuels for ethanol plants. In *Proc. Transition to a Bioeconomy: Integration of Agricultural and Energy Systems,* Atlanta, GA: Farm Foundation.

Van de Velden, M., F. Xianfeng, A. Ingram, and J. Baeyens. 2007. Fast pyrolysis of biomass in a circulating fluidized bed. *Proc. 12th Intl. Conf. on Fluidization – New Horizons in Fluidization Eng*, 896-904. Vancouver, Canada.

Wang, L., A. Kumar, C. Weller, D. Jones, and M. Hanna. 2007. Coproduction of chemical and energy products from distillers grains using supercritical fluid extraction and thermochemical conversion technologies. ASABE Paper No. 076064, Minneapolis, Minnesota: ASAE.

Waterland, L., S. Venkatesh, and S. Unnasch. 2003. Safety and performance assessment of ethanol/diesel blends (E-diesel). National Renewable Energy Laboratory. Golden, CO. Available at: http://www.nrel.gov/docs/fy03osti/34817.pdf. Accessed 28 February 2013.

Weigel, J. C., D. Loy, and L. Kilmer. 1997. Feed co-products of the dry corn milling process. Renewable Fuels Association, Washington, DC, and National Corn Growers Association, St. Louis, MO.

Table 1. Experimental design.*

Treatment	Pyrolysis Replication	Temperature (^{o}C)	Retention Time (h)	Heating Rate (^{o}C/min)
1	A / B	500	1.5	30
2	A / B	500	1.5	50
3	A / B	500	2.5	30
4	A / B	500	2.5	50
5	A / B / C	600	2	40
6	A / B	700	1.5	30
7	A / B	700	1.5	50
8	A / B	700	2.5	30
9	A / B	700	2.5	50

*Design was a 2 x 2 x 2 + 1 center point for a total of 9 treatment combinations

Table 2. Properties of resulting bio-oils.*

Treatment	Yield (%)	Thermal Diffusivity (mm^2/s)	Thermal Conductivity (W/m^oC)	Lower Heating Value (MJ/kg)
1	16.98_a	0.127_a	2.018_{ab}	21.48_a
	-0.33	-0.01	-0.16	-1.47
2	18.00_a	0.120_{ab}	1.905_a	16.71_a
	-2.16	-0.01	-0.11	-7.86
3	21.01_a	0.118_b	1.945_a	23.07_a
	-0.7	-0.01	-0.12	-0.89
4	20.56_a	0.123_{ab}	2.005_{ab}	21.96_a
	-1.51	-0.01	-0.11	-2.07
5	30.27_b	0.120_{ab}	2.328_{bc}	25.27_a
	-3.7	0	-0.13	-0.91
6	38.74_c	0.092_d	4.380_d	19.67_a
	-1.26	0	-0.45	-9.7
7	34.61_d	0.118_b	2.722_e	26.12_a
	-0.65	0	-0.2	-1.25
8	31.18_b	0.120_{ab}	2.502_{ce}	27.08_a
	-4.2	-0.01	-0.1	-2.38
9	38.18_c	0.095_d	4.230_d	27.59_a
	-1.13	-0.01	-0.93	-19.41

*Values in parentheses are standard deviation (SD). Values for bio-oils followed by the same letter (a, b, and c) within a column are not significantly different ($\alpha = 0.05$, LSD) from other treatments

Table 3. Properties of resulting bio-oils (continued).*

Treatment	Density (g/mL)	Color			pH
		L*	a*	b*	
1	0.964_{ab} (0.03)	8.258_{a} (1.37)	12.197_{a} (7.11)	4.613_{a} (1.87)	4.25_{a} (0.05)
2	0.936_{ab} (0.05)	4.422_{bc} (0.13)	8.358_{b} (0.91)	2.752_{b} (0.15)	4.55_{b} (0.09)
3	0.839_{a} (0.37)	6.173_{bd} (1.92)	9.163_{b} (0.43)	3.005_{b} (0.13)	4.28_{a} (0.01)
4	0.996_{b} (0.00)	3.357_{c} (1.28)	3.720_{c} (1.17)	1.548_{c} (0.16)	4.46_{b} (0.15)
5	1.000_{b} (0.01)	6.171_{d} (2.98)	1.469_{cd} (0.82)	1.169_{c} (0.27)	4.97_{c} (0.04)
6	0.998_{b} (0.01)	3.308_{c} (0.63)	0.645_{d} (0.09)	1.307_{c} (0.04)	5.37_{d} (0.01)
7	1.003_{b} (0.01)	4.530_{bcd} (1.51)	0.332_{d} (0.16)	1.058_{c} (0.20)	5.39_{de} (0.05)
8	1.007_{b} (0.01)	3.862_{c} (0.05)	0.382_{d} (0.04)	1.192_{c} (0.14)	5.47_{ef} (0.04)
9	1.001_{b} (0.01)	3.507_{c} (0.36)	0.330_{d} (0.25)	1.313_{c} (0.18)	5.52_{f} (0.06)

*Values in parentheses are standard deviation (SD). Values for bio-oils followed by the same letter (a, b, and c) within a column are not significantly different ($\alpha = 0.05$, LSD) from other treatments.

Table 4. Viscosity equation coefficients for bio-oils.*

Temperature	10°C		20°C		40°C	
Treatment	K	n	K	n	K	n
1	0.008_{ax} (0.00)	-0.248_{abcx} (0.15)	0.009_{ax} (0.00)	-0.351_{ax} (0.05)	0.005_{ax} (0.00)	-0.166_{abcx} (0.26)
2	0.008_{ax} (0.00)	-0.243_{abcxy} (0.06)	0.009_{ax} (0.00)	-0.351_{abcx} (0.05)	0.008_{ax} (0.00)	-0.383_{dy} (0.05)
3	0.007_{ax} (0.00)	-0.203_{abx} (0.15)	0.005_{ax} (0.00)	-0.207_{abcx} (0.11)	0.006_{ax} (0.01)	-0.227_{abcdx} (0.22)
4	0.010_{ax} (0.00)	-0.313_{abcx} (0.03)	0.011_{ax} (0.01)	-0.355_{abx} (0.17)	0.007_{ax} (0.00)	-0.295_{acdx} (0.11)
5	0.583_{ax} (0.74)	-0.741_{abcdx} (0.41)	0.056_{ax} (0.10)	-0.215_{abcy} (0.14)	0.009_{ax} (0.00)	-0.354_{cdxy} (0.12)
6	79.481_{cx} (46.10)	-0.091_{ax} (1.74)	0.928_{by} (1.12)	-0.354_{abx} (0.34)	0.073_{by} (0.04)	-0.090_{bx} (0.03)
7	17.036_{adx} (5.44)	-1.257_{dx} (0.34)	0.033_{ay} (0.01)	-0.077_{cy} (0.01)	0.011_{ay} (0.01)	-0.086_{by} (0.04)
8	3.322_{ax} (3.70)	-1.037_{bcdx} (0.53)	0.041_{ax} (0.01)	-0.064_{cy} (0.04)	0.003_{ax} (0.00)	-0.153_{abcy} (0.08)
9	49.402_{cdx} (68.59)	-1.143_{cd} (0.56)	0.105_{ax} (0.05)	-0.077_{cy} (0.04)	0.015_{ax} (0.01)	-0.109_{aby} (0.05)

*Values in parentheses are standard deviation (SD). Values for bio-oils followed by the same letter (a, b, and c) are not significantly different ($\alpha = 0.05$, LSD) from other treatments within the same temperature (i.e. columns). Values for a given bio-oil treatment followed by the same letter (x, y, and z) are not significantly different ($\alpha = 0.05$, LSD) from that same treatment across temperatures. Viscosity was defined as: $\eta = k\gamma^n$.

Table 5. GC-MS compounds present in resulting bio-oils.*

Retention Time (min)	Molecular Formula	Treatment								
		1	2	3	4	5	6	7	8	9
4.15	$C_{10}H_8$	X	X	X	X					
4.97	C_6H_{12}	X	X	X	X	X				
4.96	C_8H_{14}	X	X	X	X					
5.13	C_8H_{18}	X	X	X						
5.32	C_5H_{11}	X	X	X		X				
5.32	C_2H_5	X	X	X		X				
6.65	C_6H_{14}	X	X	X						
7.54	C_6H_6		X	X	X	X	X	X		
7.54	C_3H_3		X	X	X	X	X	X		X
9.15	C_5H_5	X	X	X	X	X				
9.44	C_6H_{12}		X	X	X	X	X	X		
11.35	C_7H_8	X	X	X	X	X		X	X	X
22.68 / 27.95	$C_{10}H_{20}$	X	X	X	X	X	X	X	X	X
23.44	$C_{14}H_{22}$		X	X		X	X		X	X
23.91	C_8H_{13}		X	X		X	X	X	X	X
24.63	C_7H_{11}			X		X		X	X	
25.43	C_8H_{16}	X	X	X	X	X	X	X		X
25.91	$C_{13}H_{28}$	X	X	X	X	X	X		X	X
28.07	C_9H_6						X	X	X	X
28.31	C_8H_{12}					X	X	X	X	X
33.20	$C_{14}H_{10}$						X	X	X	X

*X denotes presence; blank denotes absence.

Table 6. Composition of resulting bio-chars.*

Treatment	Yield (%)	Moisture (%)	DM (%)	Total N (% d.b.)	Total C (mg/L)	C:N Ratio (d.b.)	Ash (%)
DDGS	-	5.7	93.3	4.7	46.56	10.6	-
1	71.60_{ab}	2.6_{ab}	97.5_{ab}	5.5_{ab}	55.02_{a}	10.3_{a}	7.74_{a}
	(9.01)	(0.21)	(0.21)	(0.07)	(0.83)	(0.00)	(0.60)
2	77.08_{b}	2.7_{a}	97.3_{a}	5.4_{a}	54.09_{a}	10.3_{a}	7.38_{a}
	(1.31)	(0.28)	(0.28)	(0.07)	-(1.23)	(0.07)	(1.15)
3	70.23_{ab}	2.3_{bc}	97.7_{bc}	5.8_{b}	57.70_{ab}	10.2_{a}	9.28_{ab}
	(1.13)	(0.14)	(0.14)	(0.14)	(0.87)	(0.00)	(0.43)
4	69.74_{ab}	2.1_{cd}	98.0_{cd}	5.8_{b}	57.93_{ab}	10.2_{a}	8.06_{a}
	(0.34)	(0.21)	(0.21)	(0.00)	(0.01)	(0.00)	(1.32)
5	62.00_{a}	2.0_{cd}	98.0_{cd}	6.4_{c}	61.56_{c}	9.8_{b}	12.33_{b}
	(10.00)	(0.10)	(0.10)	(0.20)	(2.19)	(0.15)	(3.83)
6	43.60_{c}	$1.8d_{e}$	98.3_{d}	6.8_{de}	61.52_{bc}	9.2_{c}	24.22_{c}
	(2.19)	(0.07)	(0.07)	(0.00)	(1.05)	(0.14)	(5.92)
7	42.91_{c}	1.0_{d}	98.1_{d}	$6.9d_{e}$	60.91_{bcd}	9.2_{c}	27.17_{c}
	(0.05)	(0.07)	(0.07)	(0.21)	(2.38)	(0.28)	(6.09)
8	39.42_{c}	1.6_{e}	98.4_{e}	6.7_{d}	57.12_{ad}	8.8_{d}	33.49_{d}
	(0.15)	(0.00)	(0.00)	(0.21)	(1.76)	(0.07)	(4.43)
9	40.26_{c}	$1.8d_{e}$	98.2_{de}	7.1_{e}	64.08_{c}	9.1_{c}	33.52_{d}
	(0.80)	(0.14)	(0.14)	(0.28)	(2.74)	(0.06)	(5.36)

*Values in parentheses are standard deviation (SD). Values for bio-chars followed by the same letter (a, b, and c) are not significantly different ($\alpha = 0.05$, LSD) from other bio-char samples. DDGS is distillers dried grains with solubles; DM is dry matter; N is nitrogen; C is carbon; and d.b. is dry basis.

Table 7. Physical properties of resulting bio-chars.*

Treatment	Heating Value (MJ/kg)	Mass Density (g/cm^3)	True Density (g/cm^3)	Porosity (%)
1	23.668_{a}	0.484_{ab}	1.629_{a}	72.203_{ab}
	(1.03)	(0.00)	(0.09)	(0.02)
2	23.802_{ab}	0.475_{ab}	1.678_{a}	73.559_{a}
	(0.21)	(0.01)	(0.01)	(0.01)
3	25.558_{bc}	0.459_{ab}	1.628_{a}	73.655_{a}
	(0.31)	(0.00)	(0.03)	(0.01)
4	25.728_{c}	0.461_{ab}	1.611_{ab}	73.008_{a}
	(0.14)	(0.00)	(0.02)	(0.01)
5	29.214_{d}	0.514_{a}	1.556_{b}	70.864_{b}
	(2.16)	(0.24)	(0.04)	(0.01)
6	27.974_{d}	0.398_{b}	1.646_{a}	73.554_{a}
	(2.23)	(0.00)	(0.06)	(0.01)
7	28.746_{d}	0.403_{b}	1.771_{c}	78.142_{c}
	(0.23)	(0.00)	(0.05)	(0.01)
8	28.678_{d}	0.405_{b}	1.868_{d}	79.740_{d}
	(0.53)	(0.00)	(0.02)	(0.00)
9	28.979_{d}	0.400_{b}	1.848_{d}	79.352_{cd}
	(0.88)	(0.00)	(0.03)	(0.00)

*Values in parentheses are standard deviation (SD). Values for bio-char followed by the same letter (a, b, and c) within a column are not significantly different ($\alpha = 0.05$, LSD) from other treatments.

Table 8. Physical properties of raw materials and resulting bio-chars.*

Treatment	Particle Size			Color		
	Q3 10	Q3 50	Q3 90	L*	a*	b*
DDGS	40.0533	13.06	21.02	0.35267	1.51033	3.45167
1	0.402_{a}	1.249_{a}	3.070_{a}	9.510_{a}	0.092_{a}	0.077_{a}
	(0.08)	(0.41)	(0.97)	(0.18)	(0.08)	(0.05)
2	0.328_{b}	0.831_{bc}	2.219_{b}	9.282_{b}	0.140_{a}	0.113_{a}
	(0.03)	(0.18)	(0.43)	(0.10)	(0.11)	(0.10)
3	0.296_{bc}	0.670_{b}	1.802_{b}	9.672_{a}	0.005_{b}	-0.025_{b}
	(0.01)	(0.04)	(0.12)	(0.09)	(0.02)	(0.02)
4	0.316_{b}	0.733_{b}	1.886_{b}	9.682_{a}	0.003_{b}	0.000_{b}
	(0.02)	(0.08)	(0.34)	(0.16)	(0.01)	(0.03)
5	0.266_{c}	0.549_{c}	1.330_{c}	10.449_{c}	-0.030_{bc}	-0.020_{b}
	(0.02)	(0.06)	(0.30)	(0.27)	(0.02)	(0.01)
6	0.156_{d}	0.366_{d}	0.760_{d}	11.870_{d}	-0.057_{c}	-0.093_{c}
	(0.02)	(0.04)	(0.06)	(0.24)	(0.01)	(0.06)
7	0.144_{d}	0.352_{d}	0.744_{d}	11.628_{e}	-0.062_{c}	-0.107_{c}
	(0.01)	(0.01)	(0.04)	(0.03)	(0.02)	(0.02)
8	0.123_{d}	0.311_{d}	0.680_{d}	12.685_{f}	-0.047_{bc}	0.025_{b}
	(0.01)	(0.01)	(0.03)	(0.12)	(0.01)	(0.01)
9	0.125_{d}	0.307_{d}	0.653_{d}	12.412_{g}	-0.047_{bc}	-0.020_{b}
	(0.01)	(0.02)	(0.11)	(0.15)	(0.02)	(0.03)

*Values in parentheses are standard deviation (SD). Values for bio-char followed by the same letter (a, b, and c) within a column are not significantly different ($\alpha = 0.05$, LSD) from other treatments. The Q3 values are the volume distribution. The d50 value is the median particle size within the population, with 50% of the population greater than this size, and 50% smaller than this size. Similarly, 10% of the population is smaller than the D10 size; while 90% of the population is smaller than the D90 size.

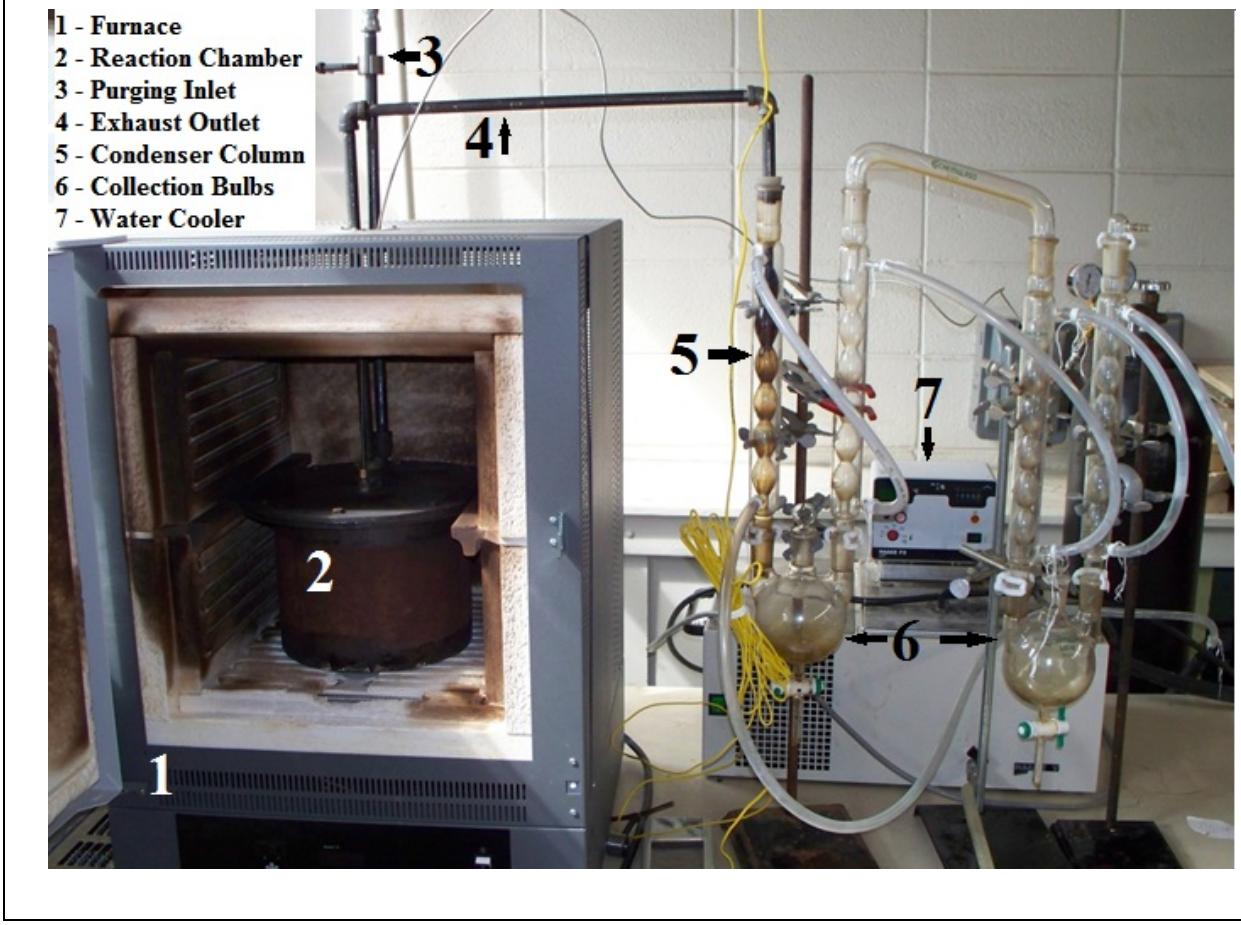

Figure 1. Pyrolysis apparatus used for this study.

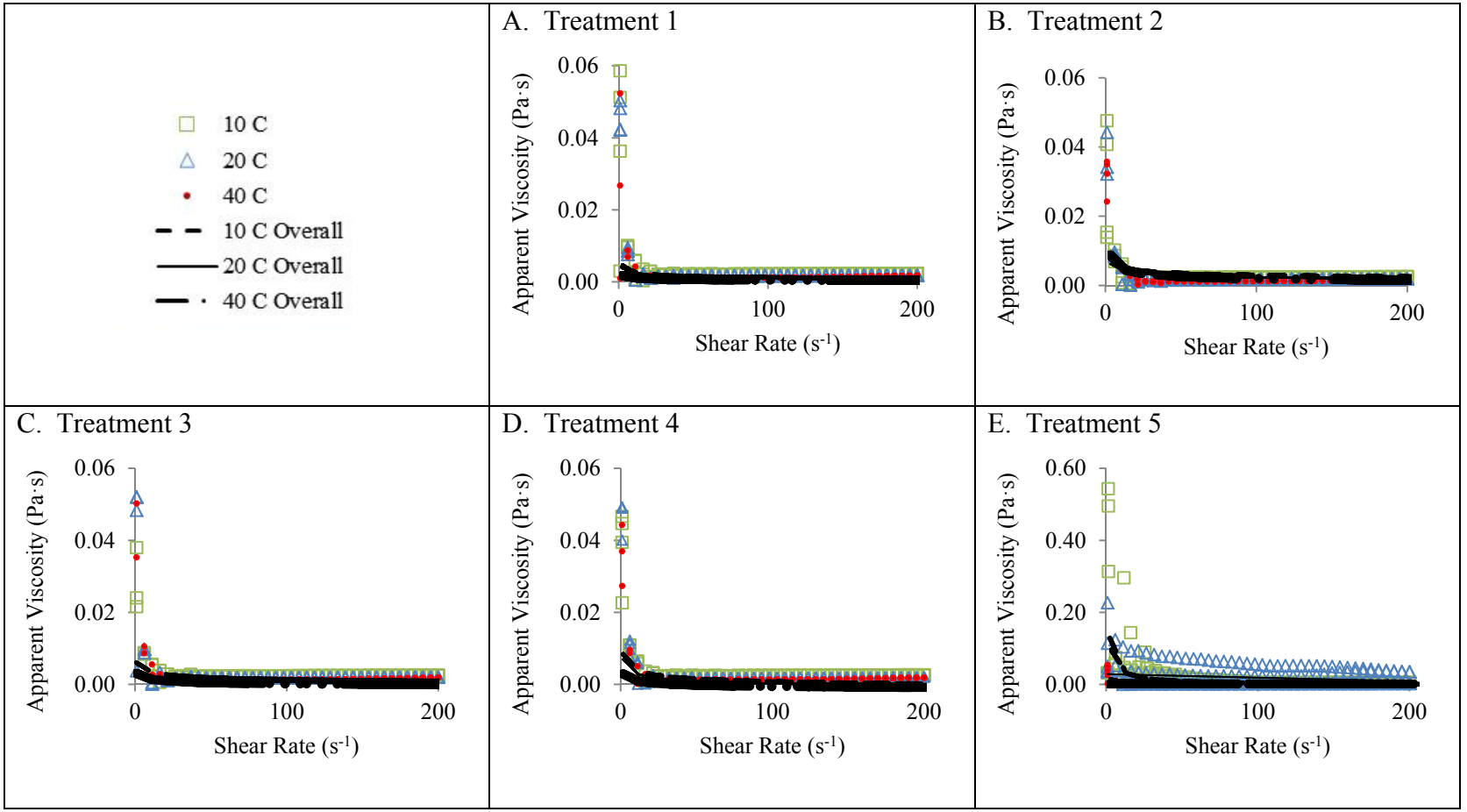

Figure 2. Relationships between apparent viscosity and shear rate as a function of temperature for the bio-oil samples. Symbols represent actual data points; lines represent regression equations. Equation coefficients are provided in Table 4.

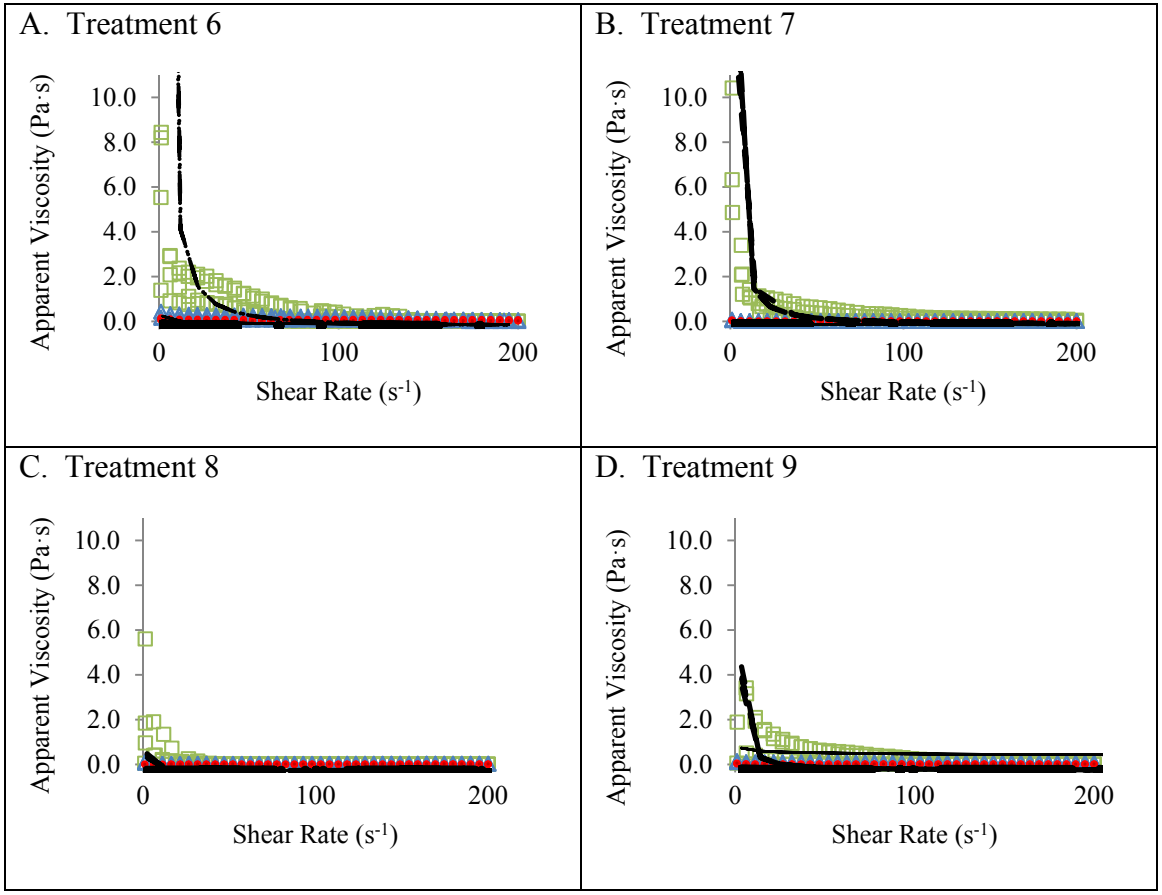

Figure 3. Relationships between apparent viscosity and shear rate as a function of temperature for the bio-oil samples (continued. Symbols represent actual data points; lines represent regression equations. Equation coefficients are provided in Table 4.